Accepted: 30 September 2019

A novel hybridized metaheuristic technique in enhancing the diagnosis of cross-sectional dent damaged offshore platform members

Wonsiri Punurai[1] | **Md Samdani Azad**[1] | **Nantiwat Pholdee**[2] | **Sujin Bureerat**[2] | **Chana Sinsabvarodom**[3]

Abstract

Offshore jacket platforms are widely used for oil and as extraction as well as transportation in shallow to moderate water depth. Tubular cross-sectional elements are used to construct offshore platforms. Tubular cross sections impart higher resistance against hydrodynamic forces and have high torsional rigidity. During operation, the members can be partially or fully damaged due to lateral impacts. The lateral impacts can be due to ship collisions or through the impact of falling objects. The impact forces can weaken some members that influence the overall performance of the platform. This demonstrates an urgent need to develop a framework that can accurately forecast dent depth as well as dent angle of the affected members. This study investigates the use of an adaptive metaheuristics algorithm to provide automatic detection of denting damage in an offshore structure. The damage information includes dent depth and the dent angle. A model is developed in combination with the percentage of the dent depth of the damaged member and is used to assess the performance of the method. It demonstrates that small changes in stiffness of individual damaged bracing members are detectable from measurements of global structural motion.

1 | INTRODUCTION

The steel jacket of an offshore structure can be designed with geometric variations in lateral bracing. Several bracing patterns such as X, D, K, V, knee-braced type provide high horizontal stiffness, ductility and redundancy to support the large gravity loads of production equipment placed on the platform deck to resist large lateral loads from wave and seismic actions. Tubular braced members are the primary structural elements used because their shapes provide high torsional rigidity and the same buckling resistance in all directions. Because of their proximity to the waterline, bracing members of the platform jackets can often fall prey to ship collisions. The inclined nature of these members makes them exposed to the objects falling from the platform deck.

Attempting to diagnose local dent-damaged tubular lateral bracing members is often a difficult task for offshore engineers. The estimation of the reduction in strength and consequences of the damage are important issues and can be assessed completely only if the information of the precise local denting damage (dent depth and dent angle) on bracing members can be exactly defined.[1-3] The denting in tubular members is a common phenomenon for older offshore structures. The reasons are pitting due to corrosion, effects from equipment, accidents due to ship collisions or dropping of heavy objects. Several methodologies and frameworks have been developed to identify the consequences due to dents in structural members. In some cases, researchers provided additional suggestions to the existing guidelines. Subsea pipelines are susceptible to face denting due to heaving lateral forces. The forces can be generated due to excavation equipment. Karamanos and Andreadakis[4] found that the presence of internal pressure influences the denting force significantly in the case of internally pressurized pipes. Cosham and Hopkins[5] explored burst strength and fatigue life for different types of dents. Burst strengths are not affected significantly by plain and smooth dents but will influence the overall fatigue life. Smooth dents along with gauges are risky for both burst strength and fatigue life. They increase the fatigue damage noticeably. Kinked dents are dangerous for longitudinal cyclic stresses. The internal pressures reduce dent length but escalate the local deformations. In the context of fixed offshore platform, finite element models have been developed and compared with the available denting test data. Storheim and Amdahl[6] suggested considering a wide variety of bows with higher vessel sizes and different bow configurations in the design of offshore structures against accidental ship collisions. The response characteristics of impact loading were presented. Cho et al[7] identified the consequences of the denting damage in tubular members in offshore structures and a relationship between dent depth and denting force was established. The damaged part geometries are illustrated mathematically for convenient beam-column analysis through proposing equations. Cho et al[8] demonstrated the response characteristics of impact loading in the context of tubular members in maritime structures. Drop tests and statistical analysis were incorporated to estimate the behavior from dynamic impact loading. The consequences of local denting and global

bending were evaluated from both experimental and numerical results. Pacheo and Durkin[9] found minor dent damages causes a major reduction of ultimate capacity. Li et al[10] reported that ship stiffness is important for impact analysis of offshore structures. Present guidelines[11] underestimate the outcome due to shipside impacts. Structures may lose all strength and collapse due to failure of a single member.[12] If the location of damage occurs in members near the sea level, the safety factor decreases significantly.[13] On the contrary, the structures become unstable if there is damage in the members close to the foundation.

Methods for direct damage detection include technology from the most conventional nondestructive tests (NDT) to high-tech three-dimensional (3D) laser scanning techniques. NDT does not need a baseline and they can be carried out locally after the damage has been located. However, for large and complex offshore platforms, it is difficult to accurately identify using these NDT techniques.[14]

Another approach is called the vibration-based damage identification technique. The technique involves the use of vibration time signals coming from acceleration sensors placed on the structure. The modal parameters (e.g., natural frequencies, mode shapes, mode shape curvatures, modal flexibility, modal strain energy, and damping ratios) can then be extracted from several measured responses. The modal parameters are functions of the physical parameters (mass, stiffness, and damping) hence existence of damage leads to changes in the modal properties of the structure. Among these data types, natural frequencies and mode shapes are widely used to combine with the feasibility of using flexibility matrix updated based, neural networks, fuzzy logic, statistical process control to obtain the element stiffness reduction in the finite element method (FEM) model of trusses, beams, and bridges.[15-19] During that process, such local modifications can indicate damage in the studied structure. In an attempt to integrate the FEM model updating into a structural damage tracking process, researchers have investigated the application of metaheuristic and evolutionary algorithms in performing FEM model updating for structural damage detection in 3D structures. For example, genetic and particle swarm optimization algorithms have been combined to model the normal (undamaged) vibration condition of structures as data clusters and then estimate a set of structural physical parameters (in the population that represents a candidate solution) that specifies the actual structural damage condition based on the learned clustered using the complementary pair of different nature-inspired optimization strategies. With this technique, the damage detection problem is treated as an inverse optimization problem where the unknown parameters of damage can be tuned automatically and accurately through the deviation minimization the norm of the difference between normal and simulated damage natural frequencies and mode shapes. Some other studies proposed well-known self-adaptive metaheuristic methods such as JADE, EGSA, PSO, sine cosine algorithm (SCA), CMAES, MARSHAL, and Success-history-based adaptive differential evolution (SHADE) to improve the optimization performance.[20-26] Recently, Bureerat and Pholdee[27] presented an adaptive SCA integrated with differential evolution to further improve its performance. The proposed adaptive sine cosine algorithm hybridized with differential evolution (ASCA-DE) algorithm is a more reliable method in the simulation experiments compared with other well-known methods. This provides the possibility of hybridizing SCA with a differential evolution (DE) technique that is efficient for structural damage detection problems. A broad- ranging application and development of metaheuristic optimizations in solving other engineering problems are demonstrated in previous studies.[28-34]

The goal of this study is to enhance dent damage detection of tubular jacket braced and leg members through an adaptive optimization algorithm. By following back to the research conducted previously, the ASCA-DE is adopted and combined with the parameter separation technique to be called as ASCA-DE-ps. The ASCA-DE-ps is used to solve the objective function

that addresses the optimization problem of dent-damaged offshore platform bracing to determine the correct geometrical parameters of dents, namely, dent depth and dent angle. For a structural damage identification problem, the changes in natural frequencies and correlation index of mode shapes from the FEM model of the intact and those measured from the dented structure are employed to develop the objective function. The proposed framework is tested against other well-established self-adaptive metaheuristics (MHs). The overall strong performance of the suggested method is maintained even in the case when two local members dent differently in both magnitude and directions.

2 | OFFSHORE STRUCTURAL MODEL DESCRIPTION

2.1 | Offshore platform

Offshore jacket platforms for oil and gas operation are deployed to conduct the adaptive metaheuristic analysis. It is adopted from Punurai et al[35] for this study. Dynamic analyses of the offshore structures are performed by using the FEM. Three-dimensional frame elements are employed to model the structural members of the platform. The jacket structure is symmetrical along both horizontal axes. The physical configurations of the jacket platform are demonstrated in Figure 1.

The jacket consists of four legs to carry the topside about 2 500 000 kg for operations in a water depth of 65.31 m as shown in Figure 2. Fixed support is adopted as a foundation system to simplify the model. The topside is modeled as a top mass to distribute over the top of the jacket legs equally. Only the jacket substructure is simplified to perform the optimization. The structural dimension of the jacket structure at the seabed is 21.76×21.76 m and at the top level is 8×8 m. The majority of the bracing systems in the jacket structures is the single brace to optimize the weight of structures except for the bottom elevation, in which K-bracing is used to compromise the connecting angle between chord and brace members of more than 30° to avoid welding problems.

The platform is designed to carry the offshore environmental loading including wind, wave, current, and payloads according to the design specifications.[36] The structural members con-

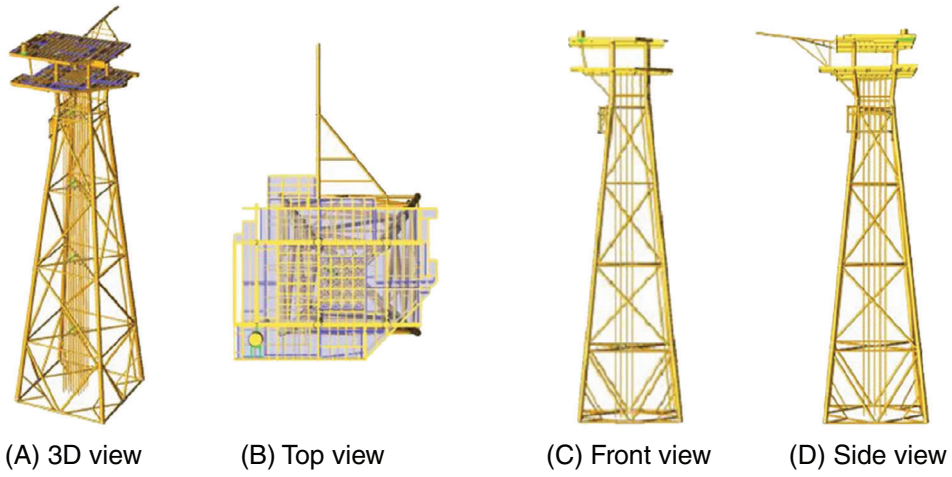

FIGURE 1 Configuration of steel jacket offshore platform in the different perspectives: A, three-dimensional view. B, top view. C, front view. D, side view

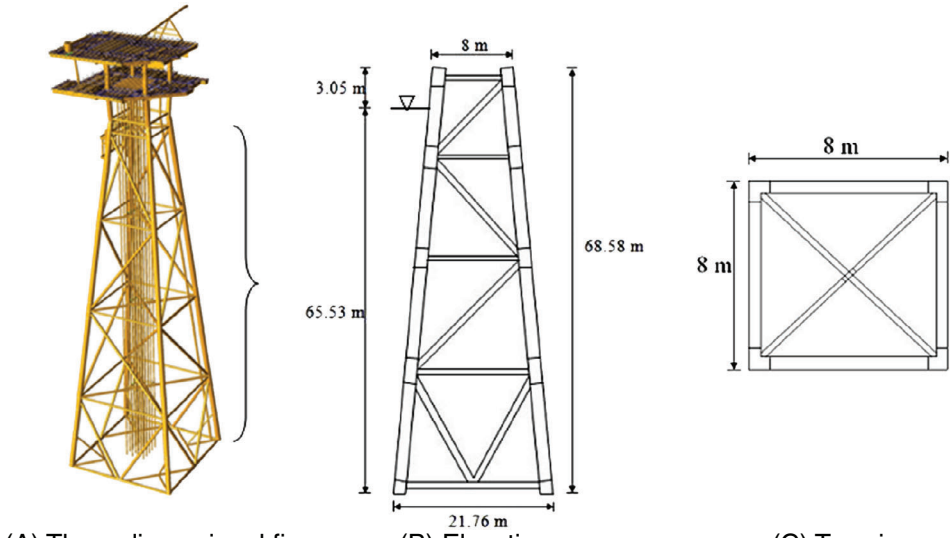

FIGURE 2 A, Three-dimensional figure. B, Elevation of jacket. C, Topside view of the jacket

TABLE 1 Specifications of structural members of jacket platform

Group	Element numbers	Outside diameter (m)	Thickness (m)	Denting in element
G1	1 to 20	1.067	0.038	5, 10, 15 and 20
G2	21 to 28	0.457	0.010	No denting
G3	29 to 32	0.406	0.013	No denting
G4	33 to 44	0.356	0.010	No denting
G5	45 to 52	0.457	0.013	No denting
G6	53 to 60; 117 to 120	0.356	0.013	No denting
G7	61 to 68	0.406	0.016	No denting
G8	69 to 72	0.324	0.010	No denting
G9	73 to 80; 85 to 92	0.559	0.013	86, 88, 90 and 92
G10	81 to 84	0.559	0.019	No denting
G11	93 to 116	0.610	0.025	No denting

sist of 11 section members as listed in Table 1. Different types of members are shown using different colors. All structural members have the same material properties as elastic modulus, $E = 205 \times 10^8$ Pa, Poisson ratio $\nu = 0.3$, steel density 7850 kg/m^3. The member group specification of offshore jacket structure is shown in Figure 3.

2.2 | The dynamic analysis of offshore structure

Free vibration analysis is incorporated to determine the natural frequencies of the offshore structures. The governing dynamic equation for the free vibration of the structure can be expressed in Equation (1).

$$\mathbf{ma} + \mathbf{cv} + \mathbf{ku} = \mathbf{0} \tag{1}$$

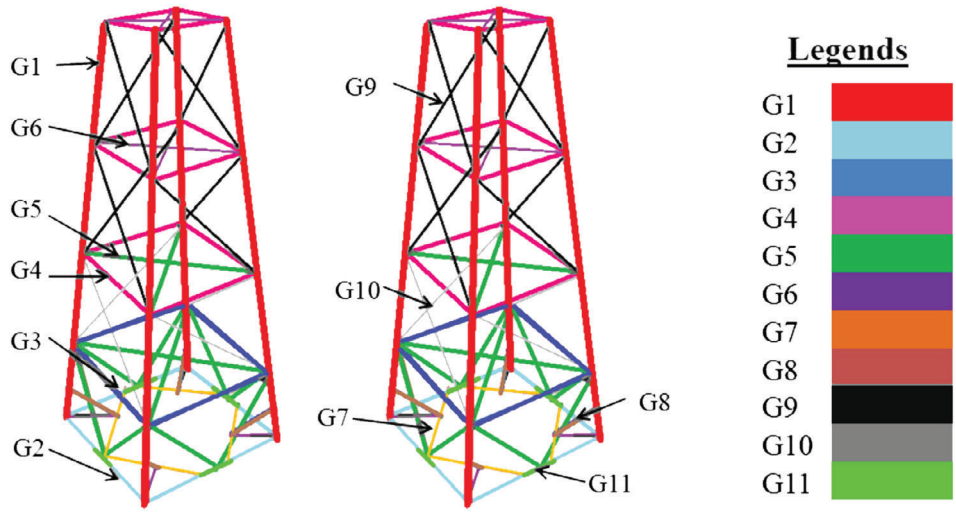

FIGURE 3 Member group specifications of jacket platform

where, m is the mass matrix, a is acceleration vector, c is the damping matrix, v is velocity vector, k is the stiffness matrix, and u is displacement vector. The mass matrix is developed following the lump mass method[37] and the stiffness matrix is derived using the direct stiffness method.[37] For finite element analysis, the eigenvalue analysis is applied to determine the natural modes of the offshore structure. The formulation is given in Equation (2).

$$[\mathbf{k} - \boldsymbol{\omega}_n^2 \mathbf{m}]\boldsymbol{\phi}_\mathbf{n} = \mathbf{0} \tag{2}$$

where ω^2 is the eigenvalue, which is associated with the natural frequency of the structures, ω rad/s, φ is the eigenvector, which demonstrates the mode shape of the structures. The calculation of the vibration response of the considered shallow water offshore platform is required for the numerical calculation and damage identification scheme based on a modified metaheuristic approach. To approximate the vibration response, a program written in MATLAB is used. For the considered identification problem, a benchmark offshore platform described in Azad et al[13] is used. The geometry and structural characteristics are taken as is from Punurai et al.[28]

2.3 | Denting data and assumptions

The local damage in the members of jacket structures typically occurs due to accident scenarios such as dropped objects or ship collisions. Structural health monitoring is significant to maintain the safety condition of the platform. Subsequently, local damages are typically presented through the dented members. Three members of the jacket structure from two different groups are assumed to be subjected to ship collisions. Member numbers 10 and 20 from G1 group and member number 88 from G9 group are the dented members. The vessel can impact the jacket platform in two directions, either in a bow or starboard direction. The location of dented members and impact directions are shown in Figure 4. Two members from the leg and one bracing member are impacted in accordance with Figure 5. Denting can be defined as the reduction of diameter from a single direction due to impact load according to the code of practices.[38]

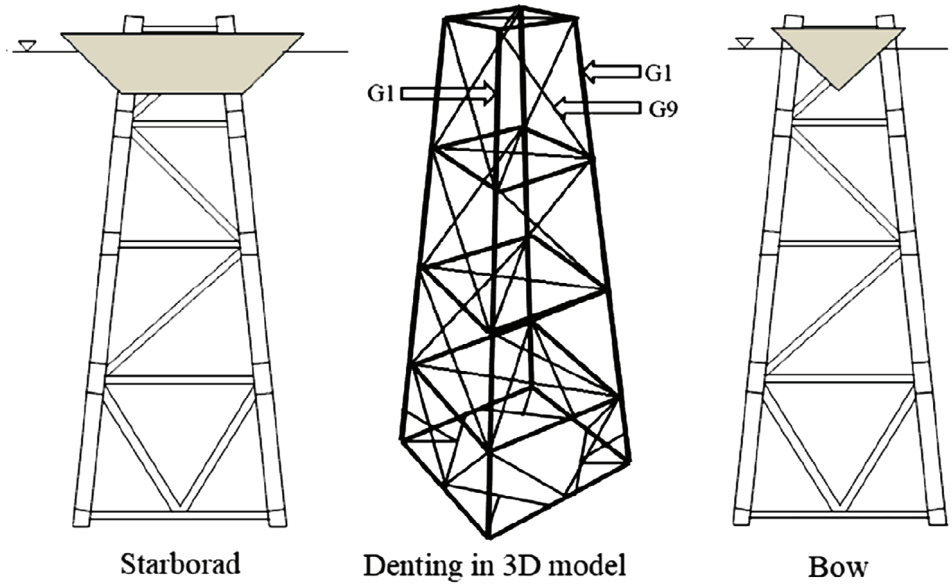

FIGURE 4 Ship collision and denting

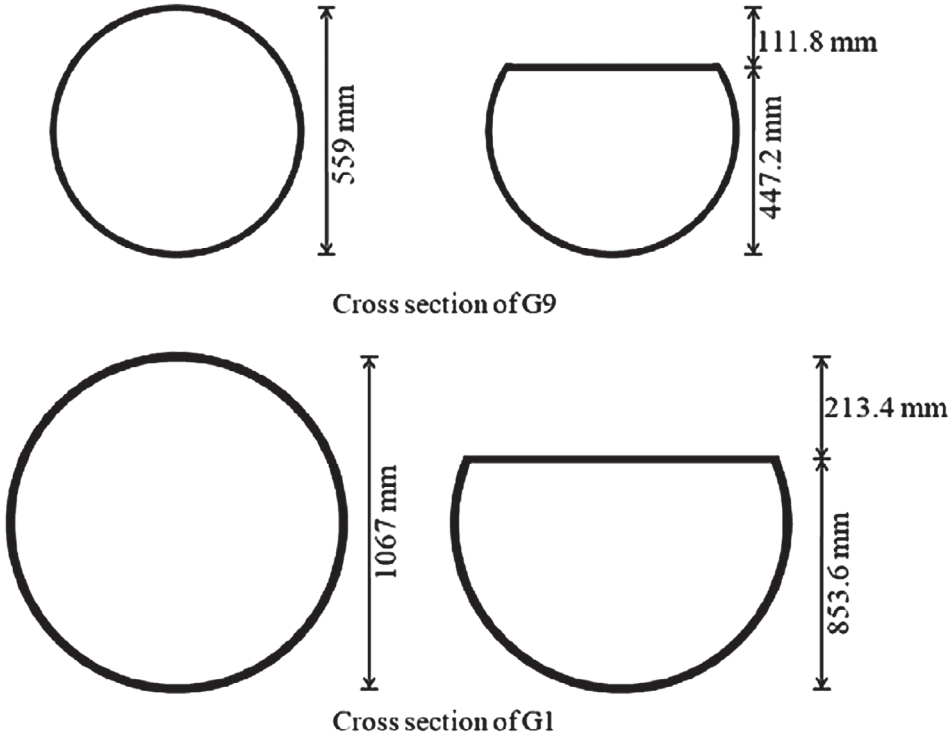

FIGURE 5 Denting of G1 and G9

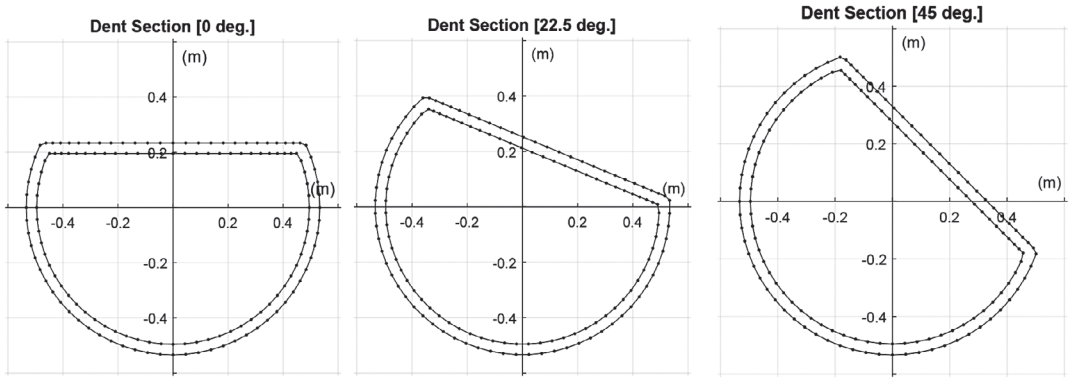

FIGURE 6 Dented members with different angles

For this research, the dented sections of jacket structures are modeled using algorithms of polygon geometry in MATLAB to estimate the sectional properties of the structural members such as area, moment of inertia, and radius of gyration.

Examples of the dented section with different angles are demonstrated in Figure 6. In this study, five different angles are adopted consisting: 0°, 22.5°, 30°, 45°, and 60°. Thirty percent denting is considered in this research. The member stiffness and cross-sectional property will be changed except member mass. A single point of the dented section will affect the whole member length and hence the cross-sectional property will be modified over the member's length. The angle of dent depth is not certain. It can occur in any direction. The denting angle can be different, based on the direction of the vessel's impact on the platform. These different directions can cause different moments of inertia about the corresponding axes. The cross-sectional area remains the same for any direction of dent depth. The cross-sectional area is only dependent on the dent depth, while moment of inertia depends on both depth and direction of impact. The angles for denting direction are also considered based on these phenomena in this study.

3 | OPTIMIZATION PROBLEM OF OFFSHORE DENT DETECTION AND NUMERICAL EXPERIMENT SETUP

In this work, vibration-based damage detection is presented for offshore health monitoring. The main concept of such damage detection is that updated mechanical properties of a mathematical model, such as a finite element model and the modal data of the model are first set to coincide with the measured data. Damage of the structure is identified by detecting changes of those mechanical properties. In this work, an optimization problem for offshore dent detection is posed to find percentages of dent in element diameters (P_{d}) and impact angles (θ) which consequently lead to changes in mechanical properties (cross-sectional areas, second moment of areas with respect to y and z directions) and natural frequencies of the offshore structure, while the objective function is to minimize root mean square error of natural frequencies and correlation index of mode shapes between measured from the dented structure and the intact structure computed by using the finite element model. The problem is expressed in Equation (3) as:

$$\mathrm{Min}\ :\ f(\mathbf{x}) = \sqrt{\frac{\sum_{j=1}^{n_{\mathrm{mode}}}\left(1-\frac{\omega_{j,\mathrm{damage}}}{\omega_{j,\mathrm{computed}}}\right)^2}{n_{\mathrm{mode}}}} + \sum_{j=1}^{n_{\mathrm{mode}}}\frac{(1-\sqrt{\mathrm{mac}_j})^2}{\mathrm{mac}_j} \tag{3}$$

TABLE 2 Natural frequency frequencies of the dented and undented structures (hz)

Mode	Undented structure	Dented structure
1	0.68	0.674
2	0.69	0.714
3	0.919	0.989
4	2.506	2.507
5	2.527	2.527
6	3.179	3.145

where $\omega_{j,\,\text{damage}}$ and $\omega_{j,\,\text{computed}}$ are the structural natural frequency of mode j obtained from a dented structure and that from the finite element model, respectively. The variable n_{model} is the number of vibration modes used. The mac is a correlation index between mode shape from the dented structure and that from the finite element model which can be calculated using Equation (4) as:

$$\text{mac}_j = \frac{|\mathbf{V}'_{\text{damage}} \times \mathbf{V}_{\text{computed}}|}{(\mathbf{V}_{\text{damage}} \circ \mathbf{V}_{\text{damage}}) \times (\mathbf{V}_{\text{computed}} \circ \mathbf{V}_{\text{computed}})} \tag{4}$$

where $\mathbf{V}_{\text{damage}}$ and $\mathbf{V}_{\text{computed}}$ are mode shapes obtained from a dented structure and that from the finite element model, respectively. $\mathbf{x}$ is design variables including percentages of dent in element diameters and impact angles ($\mathbf{x} = \{P_{\text{d1}}, P_{\text{d2}}, \dots P_{\text{dn}}, \theta_1, \theta_2, \dots, \theta_{\text{n}}\}^T$). In this work, only element numbers 5, 10, 15, 20, 86, 88, 90, and 92 which are located at the sea level are set to have dent possibilities. Therefore, the total number of design variables is set to be 16 (eight for percentages of dent and other eight for impact angles of the elements). The degrees or percentages of dent (P) are set in a range of [0, 0.7] while the possible values for the impact angle are {0, 22.5, 45}.

To investigate the search performance of optimization methods in solving the proposed optimization problem of dent detection of the offshore structure, the percentages of dent in element diameters and impact angles are predefined, while natural frequencies are simulated employing finite element analysis instead of using real measured data. The percentages of dent in element diameters and impact angles are set as 0.3% of dent at elements 10, 20, and 88 with impact angles of 0°, 22.5°, and 45°, respectively. The natural frequencies for the first six modes of the dented and undented structures are shown in Table 2.

4 | ASCA-DE AND THE PROPOSED ASCA-DE-PS TECHNIQUE

The SCA is a population-based optimization method proposed by Mirjalili.[23] The algorithm contains three main steps include an initialization phase, a reproduction phase, and a selection phase, where the reproduction phase can be performed based on sine and cosine functions. Given a current population having NP members $\mathbf{X} = \{\mathbf{x}_1, \mathbf{x}_2, \dots, \mathbf{x}_{\text{NP}}\}^{\text{T}}$, an element of a solution vector for the next generation can be calculated as follows:

$$x_{\text{new},k} = \begin{cases} x_{\text{old},k} + r_1 \sin(r_2)|r_3 x_{\text{best},k} - x_{\text{old},k}|, & \text{if } r_4 < 0.5, \\ x_{\text{old},k} + r_1 \cos(r_2)|r_3 x_{\text{best},k} - x_{\text{old},k}|, & \text{otherwise} \end{cases} \tag{5}$$

where $x_{\text{best},k}$ is the kth matrix element of the current best solution. The variables r_2, r_3, and r_4 are random parameters in the ranges of [0, 2π], [0, 2], and [0, 1], respectively. The variable r_1 is an iterative adaption parameter,

$$r_1 = a - T\frac{a}{T_{\max}} \tag{6}$$

where a is a constant parameter while T is an iteration number. $T_{\max}$ is the maximum number of iterations.

The search process of SCA starts with generating an initial population at random, and then calculating their objective function values where the best solution is found. The new population for the next generation is generated using Equation (5) and the objective function values of its members are calculated. The current best will be compared with the best solution of the newly generated population and the better one is saved to the next generation. The process is repeated until a termination criterion is met. The computational steps of SCA are shown in Algorithm 1.

Algorithm 1 Sine Cosine Algorithm

Input: population size (N_{p}), number of generations ($T_{\max}$), number of design variable (D)
Output: $\mathbf{x}_{\text{best}}, f_{\text{best}}$
Main algorithm
1: Initialize a population and set as the current population.
2: Find the best solution ($\mathbf{x}_{\text{best}}$)
3: For T=1 to $T_{\max}$
4: Calculate parameter r_1 using Equation (6)
5: For l= 1 to N_{p}
6: For k = 1 to D
7: Generate the parameter r_2, r_3, and r_4
8: Update the kth element of the lth population ($\mathbf{x}_{\text{l}}$) using Equation (5)
9: End For
10: End For
11: Calculate objective function values of the newly generated population and find the best ones ($\mathbf{x}_{\text{best,new}}$) using Equation (5)
12: Replace $\mathbf{x}_{\text{best}}$ by $\mathbf{x}_{\text{best,new}}$ if $f(\mathbf{x}_{\text{best,new}}) < f(\mathbf{x}_{\text{best}})$
13: End

The adaptive SCA with integration of DE mutation was proposed by Bureerat and Pholdee.[27] In the algorithm, the DE mutation operator as used in Pholdee and Bureerat[32] is integrated into the updating operation. The mutation equation is detailed as shown in Equation (7).

$$\mathbf{x}_{\text{new}} = \mathbf{x}_{\text{best}} + \text{rand}(-1, +1)F(\mathbf{x}_{r,1} + \mathbf{x}_{r,2} - \mathbf{x}_{r,3} - \mathbf{x}_{r,4}) \tag{7}$$

where rand (−1, 1) gives either −1 or 1 with equal probability. F is a scaling factor while $\mathbf{x}_{r,1}$–$\mathbf{x}_{r,4}$ are four solutions randomly selected from the population.

At the ASCA-DE updating operation, if a generated uniform random number in the interval [0,1] is lower than a probability value (rand < P_{DE}), the population will be updated using the SCA updating scheme based on Equation (5), otherwise, the population will be updated by DE mutation as detailed in Equation (7).

The term of self-adaption of the proposed algorithm is accomplished in such a way that the parameters r_2, r_3, and F are regenerated for each calculation based on the information from the previous iteration. For each calculation, r_2 and r_3 are generated based on normally distributed random numbers with mean values, r_{2m} and $r_{3m,}$ respectively, and standard deviation values, SD = 0.1, for both r_2 and r_3. The values of r_{2m} and r_{3m} are iteratively adapted based on the following Equations (8) and (9).

$$r_{2m}(T+1) = 0.9\, r_{2m}(T) + 0.1\ \ \text{mean}(\text{good}\ r_{2m}), \tag{8}$$

and,

$$r_{3m}(T+1) = 0.9\, r_{3m}(T) + 0.1\ \ \text{mean}(\text{good}\ r_{3m}), \tag{9}$$

where mean (good_{r2m}) and mean (good_{r3m}) are the mean values of all values of r_2 and r_3 used in the current iteration that lead to successful updates. The successful update means the created offspring is better than its parent from the previous iteration. In addition, for each calculation, the scaling factor F is generated by Cauchy distribution randomization with the mean value F_m and SD value of 0.1.[27] The F_m is iteratively adapted using the Lehmer mean defined as shown in the following Equation (10).

$$F_m(T+1) = 0.9F_m(T) + 0.1\frac{\text{sum}(\text{good}_F^2)}{\text{sum}(\text{good}_F)} \tag{10}$$

where good_F is a tray of all F used in the current iteration with successful updates.

The parameter P_{DE} is also regenerated in a similar fashion to r_2 and r_3 before updating a population. For an individual solution, the P_{DE} is generated by normal distribution randomizing with the mean value of P_{DEm} and SD of 0.1. P_{DEm} is iteratively adapted based on the following Equation (11).

$$P_{DEm}(T+1) = 0.9\, P_{DEm}(T) + 0.1\ \text{mean}\ (\text{good}\ P_{DEm}) \tag{11}$$

where good_{PDE} means all P_{DE} values used in the current iteration with successful updates. It should be note that the SD use in each parameter adaption process is set to be 0.1 based on the successful record from the previous study.[26]

The search process of ASCA-DE starts with initializing a population, r_{2m}, r_{3m}, $F_{m,}$ and P_{DEm}. The $good_{r2m}$, $good_{r3m}$, $\text{good}_{F,}$ and good_{PDE} trays are empty initially. After having calculated objective function values, the current best solution will be obtained. To firstly update a population, P_{DE} is defined and a uniform random number in [0,1] is generated. If the generated random number is lower than P_{DE}, a scaling factor (F) is generated based on F_m and a new solution is created using Equation (7), otherwise, a new solution is generated based on Equation (5). For each calculation of Equation (5), r_2 and r_3 are generated based on r_{2m} and r_{3m}. If a newly generated solution is better than its parent, the new solution will be selected for the next generation while saving all used parameters P_{DE}, r_2, r_3, and F into the good_{PDE}, good_{r2m}, good_{r3m}, and good_F trays, respectively. Then, r_{2m}, r_{3m}, F_m, and P_{DEm} are updated using Equations (8) to (11). The search process is repeated until a termination criterion is reached. The computational steps of ASCA-DE are shown in Algorithm 2.

Algorithm 2 ASCA-DE

Input: population size (N_p), number of generations (T_{max}), number of design variable (D)
Output: $\mathbf{x}_{best}, f_{best}$
Main algorithm
1: Initialize a population, r_{2m}, r_{3m}, F_m, and P_{DEm}.
2: Find the best solution ($\mathbf{x}_{best}$)
3: *For* T=1 to T_{max}
4: Calculate parameter r_1 using Equation (6)
5: Empty $good_{r2m}$, $good_{r3m}$, $good_F$, and $good_{PDE}$
5: *For* l=1 to N_p
6: Generate P_{DE} by normal distribution random with mean values P_{DEm} and SD =0.1
7: *IF rand*< P_{DE}
8: Generate F by Cauchy distribution random with mean value F_m and SD = 0.1
9: Updated a population using Equation (7)
10: *Else*
11: *For* $k = 1$ to D
12: Generate the parameter r_2 and r_3 by normal distribution random with mean values r_{2m}, r_{3m}, and SD = 0.1
13: Random generate r_4 in rank [0, 1]
14: Update the kth element of the lth population ($\mathbf{x}_l$) using Equation (5)
15: *End For*
16: *End IF*
17: Calculate objective function values of the newly generated population
18: *IF* $f(\mathbf{x}_{l,new}) < f(\mathbf{x}_{l,old})$
19: Replace $\mathbf{x}_{l,old}$ by $\mathbf{x}_{l,new}$
20: Add all generated r_2, r_3, F, and P_{DE}, into the $good_{r2m}$, $good_{r3m}$, $good_F$ and $good_{PDE}$ tray, respectively.
21: *End IF*
22: *End For*
23: Find the best solution ($\mathbf{x}_{best}$)
24: Update r_{2m}, r_{3m}, F_m, and P_{DEm} using Equation (8) to (11)
25: End

To increase the searching performance of the ASCA-DE in solving such a problem, a parameter separation technique is applied to the original ASCA-DE, denoted as ASCA-DE-ps. The search process of ASCA-DE-ps can be carried out based on a simple concept that the optimization search process of the original ASCA-DE is divided into two steps. In the first step, the original ASCA-DE is used to find only percentages of dents while the set of dent angle variables is fixed to be 0. After obtaining the optimum results from the first step, the original ASCA is applied again to find the dent angles while the percentages of dent are fixed to be the best-obtained values from the first step. Moreover, only the elements having percentages of dent higher than 1 are allowed to be the values of dent angles. This means that the design variables in the second step are equal to the number of elements which are found to have the percentages of dent from the previous calculation.

Algorithm 3 ASCA-DE-ps

Input: population size (N_p), number of generations (T_{max}), number of design variable (D)
Output: $\mathbf{x}_{best}, f_{best}$
Main algorithm
1: Set the design variables as $\mathbf{x} = \{P_{d1}, P_{d2}, \dots P_{d,n}\}^T$ while the design variables of $\{\theta_1, \theta_2, \dots, \theta_n\}$ are set to be 0.
2: Applied ASCA-DE to find $\mathbf{x} = \{P_{d1}, P_{d2}, \dots P_{d,n}\}^T$ which minimizing the Equation (3)
3: Set the design variables as $\mathbf{x} = \{\theta_1, \theta_2, \dots, \theta_n\}^T$ while the design variables of $\{P_{d1}, P_{d2}, \dots P_{d,n}\}$ are set based on $\boldsymbol{x}_{best}$ obtained from step 2.
4: Applied ASCA-DE to find $\mathbf{x} = \{\theta_1, \theta_2, \dots, \theta_n\}^T$ which minimizing the Equation (3)
5: End

5 | PERFORMANCE ASSESSMENT

To investigate the performance, the proposed technique along with six other well-established, self-adaptive MHs, the proposed technique is used to solve the optimization problem for offshore dent detection as detailed above. The MHs (details of notations can be found in the corresponding references of the methods) include:

- JADE.[20]
- SHADE.[26]
- SHADE with linear population size reduction (LSHADE).[26]
- SCA (Algorithm 1).[23]
- ASCA-DE, Algorithm 2.[27]
- SCA-ps (Algorithm 3) which replaces the ASCA-DE in step 2 and step 4 by SCA.
- ASCA-DE-ps (Algorithm 3).

Each optimizer is used to solve the offshore structure dent detection problem for 5 optimization runs. The population size is set to be 50 whereas the number of iterations is set to be 1000. All methods will be terminated with two criteria: the maximum numbers of functions evaluation as 50×1000, and the objective function value being less than or equal to 1×10^{-31}. Six vibration modes are used for calculating the objective function.

6 | RESULTS AND DISCUSSIONS

After performing 5 optimization runs of the various self-adaptive MHs for solving the proposed problem, the results are shown in Table 3. The mean and SD of the objective function are used to measure the algorithm rate of convergence and consistency in cases in which the objective function threshold (1×10^{-31}) is not reached during searching. Otherwise, the mean number of FEs and the number of successful runs out of 5 runs are used to measure the search convergence and consistency. The algorithm that is terminated by the objective function threshold is obviously superior and any run being stopped with this criterion is considered a successful run.[27]

TABLE 3 Numerical results obtained by the state of the art metaheuristics on dent detection problem

MHs	Mean objective	SD objective	Min objective	Max objective	Mean FEs	Successful runs
SCA	3.93E-06	5.27E-06	3.6E-08	9.8E-06	50 000	0
ASCA-DE	6.43E-07	1.44E-06	6.0E-23	3.2E-06	50 000	0
LSHADE	0.004667	0.004265	2.5E-04	1.2E-02	50 000	0
JADE	0.00413	0.000206	3.8E-03	4.2E-03	50 000	0
SHADE	0.005569	0.003515	3.8E-03	1.2E-02	50 000	0
ASCA-DE-ps	0	0	0	0	25 050	5
SCA-ps	6.01E-06	6.36E-06	1.9E-20	1.26E-05	50 000	0

Abbreviations: ASCA-DE, adaptive sine cosine algorithm hybridized with differential evolution; ASCA-DE-ps, ASCA-DE combined with the parameter separation; FE, finite element; JADE, adaptive differential evolution; LSHADE, SHADE with linear population size reduction; MHs, metaheuristics; SCA, sine cosine algorithm; SCA-ps, sine cosine algorithm with parameter separation; SHADE, success-history-based adaptive differential evolution.

TABLE 4 Statistical Wilcoxon rank sum test

Optimizers	SCA	ASCA-DE	LSHADE	JADE	SHADE	ASCA-DE-ps	SCA-ps
SCA	0	0	0	0	0	1	0
ASCA-DE	0	0	0	0	0	1	0
LSHADE	1	1	0	0	0	1	1
JADE	1	1	0	0	0	1	1
SHADE	1	1	0	0	0	1	1
ASCA-DE-ps	0	0	0	0	0	0	0
SCA-ps	0	1	0	0	0	1	0
Sum	3	4	0	0	0	6	3
Ranking	3	2	5	5	5	1	3

Abbreviations: ASCA-DE, adaptive sine cosine algorithm hybridized with differential evolution; ASCA-DE-ps, ASCA-DE combined with the parameter separation; JADE, adaptive differential evolution; LSHADE, SHADE with linear population size reduction; SCA, sine cosine algorithm; SCA-ps, sine cosine algorithm with parameter separation; SHADE, success-history-based adaptive differential evolution.

From Table 3, the best performer based on mean objective function values is ASCA-DE-ps while the second and the third best algorithms are ASCA-DE and SCA, respectively. When considering the number of successful runs, ASCA-DE-ps is said to be the most efficient optimizer which can detect the dent and impact angles accurately from totally 5 optimization runs with the average of 25 050 function evaluations.

In addition, the ranking of the MH optimizers was made based upon the statistical Wilcoxon rank sum test[33] as shown in Table 4. Since there are seven MHs implemented, a comparison matrix sized 7×7 whose elements are full of zeros is initially generated. The null hypothesis for the Wilcoxon rank sum test is that, for the optimization problem, the median of five objective function values obtained from method I is not different from the median of five objective function values obtained from using method J at the 5% significance level. If the null hypothesis is rejected and the median from method J is lower, the element IJ of the matrix is set to be "1." After

TABLE 5 The results on finding the percentages of dent and impact angles obtained from all MHs

Element number	Simulated dent	SCA	ASCA-DE	LSHADE	JADE	SHADE	ASCA-DE-ps	SCA-ps
10	0.3	0.3098	0.3000	0.7000	0.7000	0.7000	0.3000	0.3112
20	0.3	0.2965	0.3000	0.2393	0.5387	0.5387	0.3000	0.3009
88	0.3	0.2929	0.3000	0.1563	0.7000	0.7000	0.3000	0.2836
5	0	0.0000	0.0002	0.7000	0.7000	0.7000	0.0009	0
15	0	0.0000	0.0000	0.0005	0.7000	0.7000	0	0
86	0	0.0000	0.0007	0.2553	0.0051	0.0004	0.0003	0
90	0	0.0000	0.0000	0.0079	0.0100	0.0037	0	0
92	0	0.0000	0.0003	0.0002	0.0012	0.0001	0	0
Simulated impact angle								
10	0	0	45	0	0	45	0	22.5
20	22.5	0	45	45	22.5	45	22.50	0
88	45	0	0	0	22.5	45	45.00	22.5
5	—	45	0	22.5	45	22.5	0	0
15	—	0	45	45	22.5	45	0	0
86	—	0	0	22.5	22.5	45	0	0
90	—	0	0	0	45	0	0	0
92	—	0	0	0	45	45	0	0

Abbreviations: ASCA-DE, adaptive sine cosine algorithm hybridized with differential evolution; ASCA-DE-ps, ASCA-DE combined with the parameter separation; FE, finite element; JADE, adaptive differential evolution; LSHADE, SHADE with linear population size reduction; MHs, metaheuristics; SCA, sine cosine algorithm; SCA-ps, sine cosine algorithm with parameter separation; SHADE, success-history-based adaptive differential evolution.

summing up all values in the matrix columns, the best optimizer is the one that has the highest score. The summation and the ranking are also given in the table. Based on this assessment, the best performer is still ASCA-DE-ps while the second best is ASCA-DE. The SCA and SCA-ps algorithms have the same ranking which is the third best while LSHADE, JADE and SHADE also have the same ranking as the fifth best. This implies that there is no significant difference between SCA and SCA-ps and there is also no significant difference between LSHADE, JADE, and SHADE.

Table 5 shows the best results on finding the percentages of dent and impact angles obtained from all optimizers while Figure 7 shows their search history. From Table 4, ASCA-DE-ps can correctly detect both the percentages of dents and impact angles, while ASCA-DE, SCA, and SCA-ps can correctly detect both the percentages of dents in the offshore structure. The others failed to achieve such results. The search history from Figure 7A shows that there are two groups of optimizers. The first group converged to approximately 0.005 while the other group converged to the desired value that is near zero. When zooming into the figure as shown in Figure 7B, the optimizers which converged to approximately 0 are SCA, ASCA-DE, ASCA-DE-ps, and SCA-ps.

Overall, it was found that ASCA-DE-ps is the most efficient optimizer for solving the proposed problem. The self-adaptive scheme is said to be advantageous as it requires no

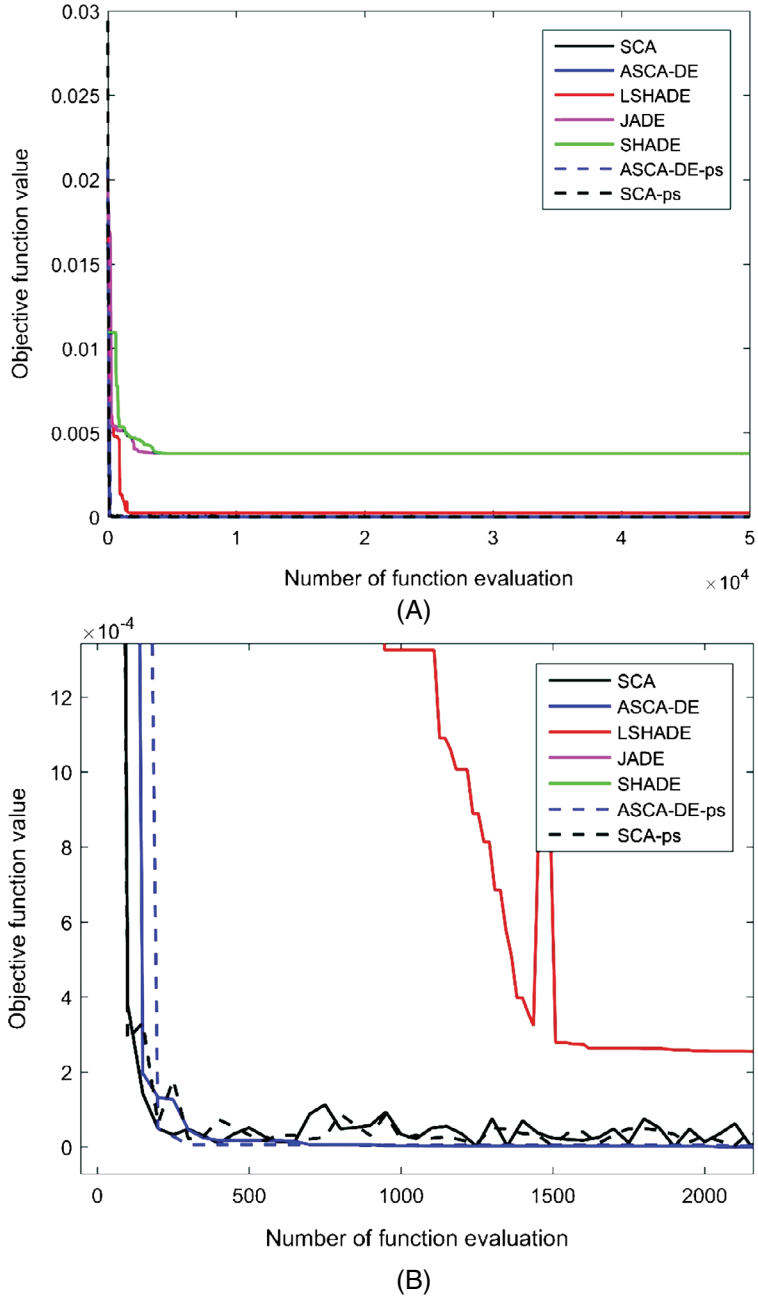

FIGURE 7 Search histories of ASCA-DE-ps as the best found objective function vs number of function evaluations A, Overall. B, Zoom in

optimization parameter settings, and results in increased convergence speed. Applying a parameter separation technique into the algorithms leads to increase in search performance. The application of the technique on a case study cannot provide reliable information about the broader problem, but it would be useful in the preliminary stages of an investigation. More should be tested systematically with a larger number of cases. Conclusion on advantages and disadvantages of the proposed ASCA-DE-ps is provided in Table 6.

TABLE 6 Conclusion on advantage and disadvantaged of the proposed ASCA-DE-ps

Advantage	Disadvantage
No optimization parameter settings required.	Using successive history-based self-adaption may reduce the algorithm search exploration.
High convergence rate for the proposed problem.	
High consistency for the proposed problem.	The performance may not guarantee for other optimization problems having higher number of design variables, highly nonlinear, and nonconvex.
High accuracy for the proposed problem which is an inverse optimization problem.	

7 | CONCLUSION

This paper describes the implementation of a new strategy for the optimizer incorporated with FE model updating used for finding the percentages of dents and impact angles of offshore platform members. The proposed method applied to the model test structure and is particular effective in the case of localization of dent damage occurring simultaneously in jacket legs and diagonal braces after impacts or ship collisions. Moreover, good results are obtained with accuracy and lower computational time. Further, research is planned to extend the proposed ASCA-DE-ps with additional assumptions for the probability density function of variables and considers its use for practical deteriorating systems imposed uncertainties. In addition, taking into account the noisy environment and the absence of complete mode shapes would confirm the reliability and validity of the proposed technique for future structural health monitoring and damage localization activities in offshore and wind turbine structures.

ACKNOWLEDGMENTS

The study was supported by Mahidol University and the European Union's Horizon 2020 research, innovation under the Marie Skłodowska-Curie grant agreement No. 730888, and Thailand Research Funds (RTA6180010).

ORCID

Wonsiri Punurai https://orcid.org/0000-0003-1260-084X

REFERENCES

1. Ellinas CP, Walker AC. Effects of damage on offshore tubular members. Paper presented at: IABSE Colloquium on Ship Collision with Bridges and Offshore Structures; 1983; Copenhagen, Denmark.
2. Yu Z, Amdahl J. Analysis and design of offshore tubular members against ship impacts. *Mar Struct*. 2018;58:109-135.
3. DNVGL-RP-C204. *Design against accidental loads*. Det Norske Veritas: Oslo, Norway; 2017:113.
4. Karamanos SA, Andreadakis KP. Denting of internally pressurized tubes under lateral loads. *Int J Mech Sci*. 2006;48(10):1080-1094.
5. Cosham A, Hopkins P. The effect of dents in pipelines—guidance in the pipeline defect assessment manual. *Int J Press Vessel Pip*. 2004;81(2):127-139.

6. Storheim M, Amdahl J. Design of offshore structures against accidental ship collisions. *Mar Struct*. 2014;37:135-172.
7. Cho SR, Kwon JS, Kwak DI. Structural characteristics of damaged offshore tubular members. *J Ocean Eng Technol*. 2010;24(4):1-7.
8. Cho SR, Le DNC, Seo BS. Response of tubular structures under dynamic impact loadings. Paper presented at: Proceedings of SNAK Autumn Conference; 2015; Geoje, SG: Society of Naval Architects of Korea.
9. Pacheco LA, Durkin S. Denting and collapse of tubular members—a numerical and experimental study. *Int J Mech Sci*. 1988;30(5):317-331.
10. Li L, Hu Z, Jiang Z. Plastic and elastic responses of a jacket platform subjected to ship impacts. *Math Probl Eng*. 2013;2013:1-15. https://doi.org/10.1155/2013/790586.
11. NORSOK Standard N–004. *Design of Steel Structures*. Lysaker, Norway: Norsok standard; 2004 287 p.
12. Golafshani AA, Tabeshpour MR, Komachi Y. FEMA approaches in seismic assessment of jacket platforms (case study: Ressalat jacket of Persian Gulf). *J Constr Steel Res*. 2009;65(10-11):1979-1986.
13. Azad MS, Punurai W, Sinsabvarodom C, Asavadorndeja P. Effects of redundancy in bracing systems on the fragility curve development of steel jacket offshore platform. *Eng J*. 2019;23(1):123-133.
14. Pedersen AT, Montes BF, Pedersen JE., Harris M, Mikkelsen T. Demonstration of short-range wind lidar in a high-performance wind tunnel. Paper presented at: EWEA 2012-European Wind Energy Conference & Exhibition; 2012; Copenhagen, Denmark.
15. Doebling SW, Farrar CR, Prime MB. A summary review of vibration-based damage identification methods. *Shock Vibrat Dig*. 1998;30(2):91-105.
16. Farrar CR, Worden K. *Structural Health Monitoring: A Machine Learning Perspective*. Chichester, UK: John Wiley & Sons; 2012 667 p.
17. Chandrashekhar M, Ganguli R. Damage assessment of structures with uncertainty by using mode-shape curvatures and fuzzy logic. *J Sound Vib*. 2012;326(3-5):939-957.
18. Jiao Y, Liu H, Cheng Y, Gong Y. Damage identification of bridge based on Chebyshev polynomial fitting and fuzzy logic without considering baseline model parameters. *Shock Vibrat*. 2015;2015:10. https://doi.org/10.1155/2015/187956.
19. Alavi AH, Hasni H, Lajnef N, Chatti K, Faridazar F. An intelligent structural damage detection approach based on self-powered wireless sensor data. *Automat Construct*. 2016;62:24-44.
20. Zhang J, Sanderson AC. JADE: adaptive differential evolution with optional external archive. *IEEE Trans Evolut Comput*. 2009;13(5):945-958.
21. Jiang SF, Fu C, Zhang C. A hybrid data-fusion system using modal data and probabilistic neural network for damage detection. *Adv Eng Softw*. 2011;42:368-374.
22. Pal J, Banerjee S. A combined modal strain energy and particle swarm optimization for health monitoring of structures. *J. Civ. Struct Health Monit*. 2015;5:353-363.
23. Mirjalili S, Lewis A. The whale optimization algorithm. *Adv Eng Softw*. 2016;95:51-67.
24. Hansen MC, DeFries RS, Townshend JR, Carroll M, DiMiceli C, Sohlberg RA. Global percent tree cover at a spatial resolution of 500 meters: first results of the MODIS vegetation continuous fields algorithm. *Earth Interact*. 2003;7(10):1-15.
25. Jahjouh M, Nackenhorst U. A modified metaheuristic optimization approach on the structural identification and damage detection of an experimentally tested wind turbine supporting structure. *Proc Appl Math Mech*. 2016;16(1):691-692.
26. Tanabe R, Fukunaga AS. Improving the search performance of SHADE using linear population size reduction. Paper presented at: IEEE Congress on Evolutionary Computation (CEC); 2014; Beijing, China.
27. Bureerat S, Pholdee N. Adaptive sine cosine algorithm integrated with differential evolution for structural damage detection. Paper presented at: International Conference on Computational Science and Its Applications; 2017; Trieste, Italy.
28. Bureerat S, Pholdee N. Optimal truss sizing using an adaptive differential evolution algorithm. *J Comput Civil Eng*. 2016;30(2):1-14. https://doi.org/10.1061/(ASCE)CP.1943-5487.0000487.
29. Pholdee N, Bureerat S. Comparative performance of metaheuristic algorithms for mass minimisation of trusses with dynamic constraints. *Adv Eng Softw*. 2014;75:1-13.
30. Ganesan T, Vasant P, Elamvazuthi I. *Advances in Metaheuristics: Applications in Engineering Systems*. Abingdon, UK: CRC Press; 2016 213 p.

31. Vasant P, Kose U, Watada J. Metaheuristic techniques in enhancing the efficiency and performance of thermo-electric cooling devices. *Energies*. 2017;10(11): 1703):1-50. https://doi.org/10.3390/en10111703.
32. Zelinka I, Tomaszek L, Vasant P, Dao TT, Hoang DV. A novel approach on evolutionary dynamics analysis–a progress report. *J Comput Sci*. 2018;25:437-445. https://doi.org/10.1016/j.jocs.2017.08.010.
33. Vasant P, Marmolejo JA, Litvinchev I, Aguilar RR. Nature-inspired metaheuristics approaches for charging plug-in hybrid electric vehicle. *Wireless Netw*. 2019;1-14. https://doi.org/10.1007/s11276-019-01993-w.
34. Tamouk J, Acan A. A multimetric and multideme multiagent system for multiobjective optimization. *Comput Intell*. 2018;34:1122-1154. https://doi.org/10.1111/coin.12175.
35. Punurai W, Azad MS, Pholdee N, Sinsabvarodom C. Adaptive metaheuristic to predict dent depth damage in the fixed offshore structures. Paper presented at: Proceedings of International European Safety and Reliability Conference (ESREL); 2018; Trondheim, Norway.
36. DNVGL-RP-C203. *Fatigue design of offshore steel structures*. Det Norske Veritas: Oslo, Norway; 2016 215 pp.
37. Logan DL. *A First Course in the Finite Element Method*. Cengage Learning: Boston, MA; 2011 1000 pp.
38. ISO 19901-3. *Petroleum and Natural Gas Industries – Specific Requirements for Offshore Structures – Part 3: Topsides Structure*. Geneva, Switzerland: International Organization for Standardization; 2014 117 pp.